Evaluation of Alternate Propellants for Pulsed Plasma Thrusters*†

Eric J. Pencil and Hani Kamhawi
National Aeronautics and Space Administration
Glenn Research Center
21000 Brookpark Road
Cleveland, OH 44135
(216) 977-7463
Eric.Pencil@grc.nasa.gov

Lynn A. Arrington
QSS Group, Inc.
Cleveland, Ohio

William Blaise Warren
University of Virginia
Charlottesville, Virginia

IEPC-01-147

Nominal, high-density, porous, and carbon-impregnated Teflon were evaluated as potential propellants in an ablative pulsed plasma thruster (PPT). PPT discharge current waveforms, ablation rates, steady-state thrust, and impulse bit per pulse were measured for selected propellants over a range of number of pulses and discharge energies. Ablation rates for nominal Teflon ranged from 4.5 to 74.1 μg/pulse for energy levels ranging from 5 to 60 joules, respectively. Application of a least square linear fit to the ablation data resulted in a slope of 1.37 μg/joule for nominal Teflon, 1.37 μg/joule for high-density Teflon, 1.88 μg/joule for porous Teflon, and 1.12 μg/joule for 2%-carbon Teflon. The thrust and single impulse-bit magnitudes at a given energy for all the propellants evaluated were within ±10% over the range of energies tested. For nominal Teflon and high-density Teflon, efficiency ranged from 6 to 12%, for porous Teflon efficiency ranged from 7 to 13%, while for 2%-carbon Teflon efficiency ranged from 6 to 18%. Analysis of experimental results using zeroth-order slug modeling indicates that carbon-impregnated Teflon has the highest fraction of its ablated mass accelerated electromagnetically.

Introduction

Pulsed plasma thrusters (PPTs) are low power electric propulsion devices, which have the unique features of low impulse bit operation combined with a high specific impulse. The solid propellant, Teflon,™ eliminates the complexities of leaky valves or pressurized vessels inherent with gas-fed systems. The inert propellant simplifies storage and handling requirements during integration with the spacecraft. The propellant feed system is inherently simple and reliable due to its single moving mechanical part, a spring. The technology has a heritage from applications stemming back to the 1960's [1]. The applications ranged from control propulsion for larger satellites to primary propulsion for small satellites. PPT features combine to offer a favorable solution to NASA's near-term and long-term deep space interferometry propulsion requirements [2, 3].

Interest in pulsed plasma thruster technology was rekindled in the mid-1990s with the development of the Earth Observing-1 (EO-1) PPT flight experiment [4]. The project was a focused development effort, which incorporated advances in power electronics and materials into existing thruster system designs. As an experiment, the EO-1 PPT was designed to replace the function of the pitch-axis control system. However, the potential use of PPTs for formation-flying applications require longer-life components and lower system mass to meet mission requirements.

* Presented as Paper IEPC-01-147 at the 27th International Electric Propulsion Conference, Pasadena, CA, 15-19 October, 2001.
† This paper is declared a work of the U.S. Government and is not subject to copyright protection in the United States.

Teflon is a trademark name of DuPont.

Application of PPTs to orbit raising maneuvers of power-limited spacecraft require higher performance than has been previously demonstrated.

One area of PPT development, which has received limited attention, is the use of alternate propellants to improve and enhance thruster performance. Replacement of the baseline Teflon propellant offers a low-risk option to thrust performance improvements. This study investigated various materials as propellants in a PPT including various density (porosity) Teflon and carbon-impregnated Teflon. Ablation rates were measured as a function of pulse energy and number of pulses. PPT discharge current waveforms were measured for all conditions and used to calculate circuit parameters. Steady-state thrust and impulse bit per pulse were measured for selected propellants over a range of thruster energies. Performance parameters such as specific impulse and efficiency were calculated and analyzed. Using a 'slug' model, the electromagnetic (EM) thrust component and propellant fraction which was electromagnetically accelerated were calculated and analyzed.

Test Apparatus and Procedures

Propellants

The propellants used in this study include nominal Teflon, porous Teflon, high-density Teflon, and carbon-impregnated Teflon. Specifically nominal Teflon, porous Teflon with 100-μm and 500-μm void sizes, high-density Teflon, and Teflon impregnated with various amounts of carbon (2%, 10%, 15%, and 25% by weight) were studied.

Porous Teflon was chosen because it allows the investigation of the effects of changing the propellant diffusivity on the thruster performance. The lower density of porous Teflon results in a higher thermal diffusivity ($\alpha=k/\rho C_p$), when compared to nominal Teflon, which increases its thermal diffusion depth ($\delta=(\alpha t)^{1/2}$). The density of selected propellants is provided below:

Propellant	Density (kg/m^3)
Nominal Teflon	2116.10
High-density Teflon	2176.00
100-μm porous Teflon	1159.43
500-μm porous Teflon	871.99
2%-carbon Teflon	2113.67

Carbon-impregnated Teflon was chosen because it allows the investigation of effect of the addition of carbon molecules on the ablation process. The addition of carbon molecules is known to change the soft radiation depth into the propellant surface and potentially reduce macroparticle ejection [5]. Carbon-impregnated Teflon is made by mixing a prescribed percentage by weight of carbon with the Teflon powder and then compressing and sintering the mixture.

Laboratory PPT

A single channel parallel plate thruster was fabricated similar to an EO-1 configuration as shown in Figure 1. This configuration provides a low impedance discharge characteristic. A Maxwell 33.2 μF oil-filled capacitor was used in this study. The thruster transmission lines and electrodes (2.54 cm long and 2.54 cm wide [6]) were fabricated from oxygen-free copper. The gap between the electrodes was 3.81 cm. The spark plug used to initiate the discharge was a Unison 1.27 cm diameter spark plug that was used in conjunction with a Unison TGLN-28 ignitor exciter circuit. The pulse repetition rate for the spark plug was typically 1 hertz. The spark plug was inserted in the cathode electrode.

The PPT discharge current waveform was measured via a Rogowski coil that is potted around the capacitor's positive lead. The output from the Rogowski coil was integrated with an RC integrator. The output of the integrator was recorded on a digitizing oscilloscope.

Ablation Rate Tests

PPT ablation rate tests were performed in an oil-diffusion pumped vacuum facility (CW-19). Typical facility base pressure was 0.1 mPa (1 μTorr). The goal of the PPT ablation rate tests was to determine a representative mass loss per pulse for the different propellants at different PPT operating energies. Propellant bars were weighed before and after testing with an electronic balance, which has an accuracy of 0.1 mg. Initial testing was performed to determine the total number of pulses required to achieve a steady-state ablation rate as well as to determine the test-to-test variation. For selected propellants, ablation rates were obtained for approximately 1000, 2000, and 5000 pulses at a pulse energy of 40 joules. Based on the initial results, all subsequent ablation rate tests for 5, 10, 20, 30, 40, and 50 joules were conducted with

approximately 5000 pulses. The tests for 60 joules were limited to 2000 pulses due to prevent excessive capacitor heating.

Concurrent to the ablation rate test, the PPT discharge current waveform, measured by a Rogowski coil, was recorded and stored via a digitizing oscilloscope. Several waveforms were recorded for each operating condition to investigate shot-to-shot variation.

Thrust Measurement Tests

A torsional-type thrust stand, located in a 1.5-meter diameter by 4.5-meter long oil-diffusion pumped vacuum facility (VF-3), shown in Figure 2, was used to perform thrust measurements. The facility base pressure was typically 0.1 mPa (1 μTorr). The thrust stand can be used to determine impulse bit and thrust as a function of thrust stand deflection, spring stiffness, and natural frequency. In-situ calibration weights were used to apply a known force to determine the deflection of the thrust stand. Both steady-state and single pulse operation can be used to determine impulse bit. Additional details for the thrust stand can be found in reference [7].

The impulse bit per shot was averaged for ten pulses to examine shot-to-shot variation in the thruster performance. The steady-state thrust was measured by operating the thrust continuously for 2 two-minute intervals. Both the single pulse impulse bit and steady state thrust were measured at each capacitor energy with each propellant.

Results, Analysis and Discussion

Ablation Rate Test

Initial testing was performed to determine the total number of pulses required to achieve a steady-state ablation rate. For selected propellants, ablation rates were obtained for approximately 1000, 2000, and 5000 pulses at a pulse energy of 40 joules. Results for these tests (and all subsequent ablation rate tests) are tabulated in Table I. Figure 3 presents ablation rates for different test duration for the different propellants at 40 joules. For all propellants, the ablation rate was lowest at 1000 pulses and increased for 2000 pulses and asymptoted at 5000 pulses. Hence, it was decided to perform all subsequent ablation rate tests at approximately 5000 pulses except for the 60 joules cases where testing was limited to 2000 pulses due to prevent excessive capacitor heating.

For nominal and 2%-carbon-impregnated Teflon ablation rate tests were repeated at least twice at 40 joules for the 5000 pulses to verify the repeatability of the ablation rate measurements. For nominal Teflon ablation rate was 52, 54.3, 54.6, and 52.9 μg/pulse for 5849, 5260, 5361, and 5105 pulses, respectively, whereas, for the 2%-carbon-impregnated Teflon ablation rates were 44.5 and 42.6 μg/pulse for 5508 and 5554 pulses, respectively. This indicated a variation of less that 5% in ablation rate.

For all propellants, the ablation rate was directly proportional to the discharge energy. For nominal Teflon, ablation rates ranged from 4.52 μg/pulse at 5 joules to 74.1 μg/pulse at 60 joules. Applying a linear least square fit to the data presented in Figure 4, it is found that the slope of the line is 1.33 μg/joule. For high-density Teflon, ablation rates ranged from 5.31 μg/pulse at 5 joules to 76.98 μg/pulse at 60 joules. Applying a least square linear fit to the data presented in Figure 4, it is found that the slope of the line is 1.37 μg/joule.

The first porous Teflon propellant tested was the 500-μm porous Teflon, which had the lowest density. For 500-μm porous Teflon ablation rates ranged from 2.96 μg/pulse at 5 joules to 94.81 μg/pulse at 50 joules. Applying a least square linear curve fit to the presented in Figure 4 for energy levels from 5 to 50 joules, it is found that the slope of the line is 1.88 μg/joule. It is also important to note here that ablation rate at 60 joules was equal to 94.59 μg/pulse which is equal to the ablation rate at 50 joules, hence, the ablation rate at 60 joules was not included in the data used in the linear fit equation. Given the time constraints of the test program and the fact that the 500-μm porous Teflon demonstrated worse performance than nominal Teflon, it was decided not to test 100-μm porous Teflon.

Propellant evaluation included testing of carbon-impregnated Teflon propellants. Propellants tested contained 2%, 10%, 15%, and 25% by weight of carbon–impregnated in the Teflon propellant bar. It is important to note that for the 2%-carbon-impregnated Teflon, the PPT discharge current had a substantial shot-to-shot variation for the 5 and 10 joules tests. As a result that data is not very reliable and was not used in subsequent calculations. Applying a linear least square fit to the data presented in Table I and Figure 4,

it is found, for the 2%-carbon-impregnated Teflon, that the slope of the line is 1.12 μg/joule.

For the 10%-carbon Teflon, initial testing was performed at 40 joules. A series of ablation rate tests were conducted at 1285, 2097, 2098, 5465, and 5591 pulses. Results showed that ablation rates varied by about 50% between the different tests. In addition, monitoring of the PPT discharge current waveform indicated that the peak current magnitudes varied by up to 40% between different pulses for a given test, this variation in the discharge current magnitude might indicate premature breakdown mainly due to the higher carbon content in the Teflon fuel bar. As a result it was decided not to further test the 10% carbon-impregnated Teflon at the other energies.

For the 15%-carbon Teflon, initial testing was conducted at 40 joules, 15 minutes into the test the PPT started to breakdown prematurely. Subsequent inspection of the thruster showed no evidence of an alternate breakdown path other than on the Teflon surface, indicating premature breakdown due to elevated carbon content in propellant bar. Finally, for the 25%-carbon fuel, the PPT capacitor could not be charged to 1550 volts due to premature breakdown on the propellant surface due to the high content of carbon.

Thrust Measurement Test

The results of the thrust measurement tests are listed in Table II. The impulse bit for all propellants are plotted as a function of discharge energy in Figure 5. Comparison of the impulse bit computed from single shot and continuous operation was used to verify the consistency of the results. For all cases, except 2%-carbon-impregnated Teflon below 20 joules and other propellants at 5 joules, both impulse bits agreed to within 5%. The impulse bit increased as the discharge energy increased for all propellants. For almost all cases, there was no measurable difference between the impulse bit measured for each propellant at a given energy. The only exception is the data point for 2%-carbon-impregnated Teflon at 20 joules. Deviation due to shot-to-shot variation of the impulse bit was calculated and used as error bars in Figure 5.

The specific impulse for each propellant was calculated and is listed in Table II using the following equation:

$$I_{sp} = \frac{I_{bit}}{Mg} \tag{1}$$

where I_{sp} is the specific impulse, I_{bit} is the impulse bit per pulse, M is the ablation rate, and g is the gravitational constant. The specific impulses are plotted as a function of discharge energy in Figure 6. In general, the specific impulse increased as discharge energy increased above a discharge energy of 10 joules. Values for specific impulse for nominal and high-density Teflon were similar, which was expected given that both ablation rates and impulse bits were the same in earlier discussion. Specific impulse for porous Teflon was lower than nominal Teflon, since porous Teflon ablated at a higher rate, but still only produced the same impulse bit as nominal Teflon. Specific impulse for 2%-carbon-impregnated Teflon was higher than nominal Teflon since the 2%-carbon-impregnated Teflon ablated at a lower rate, while producing the same impulse bit as nominal Teflon.

The efficiencies for the various propellants were calculated with the equation below and listed in Table II:

$$\eta = \frac{I_{bit}^2}{2ME} \tag{2}$$

where η is the PPT efficiency, I_{bit} is the impulse bit per pulse, M is the ablation rate, and E is the discharge energy. The efficiencies are plotted as a function of discharge energy in Figure 7. In all cases, the efficiency increases as a function of discharge energy, which is a normal trend in PPT performance. The remaining trends can be extrapolated from the results previously discussed. Given the discharge energy was held constant and the impulse bit was determined to be approximately constant for all propellants, the efficiency was inversely proportional to the ablation rate. The efficiency for nominal Teflon and high-density Teflon were the same. In addition the efficiency of the porous Teflon was lower than nominal Teflon and the efficiency of the 2%-carbon Teflon was higher than nominal Teflon.

Current Measurements and Electromagnetic Thrust Component Analysis

PPT discharge current waveforms for nominal Teflon are plotted for the various capacitor energies and are presented in Figure 8. The waveforms show an under-damped sinusoidal RLC current. PPT peak current increased as the capacitor energy increased and ranged from 5 kA at 5 joules to 30 kA at 60 joules. Typically,

the current pulse had a period of 10 μsec. PPT circuit parameters were calculated from the PPT current waveforms. Inductance values ranged between 50 and 60 nH for all energies, while resistance values ranged from 35 mΩ at 5 joules to 23 mΩ at 60 joules.

A zeroth-order slug analysis was performed to estimate fraction of the ablated mass that is accelerated electromagnetically. Assuming the discharge can be modeled as a sheet that was accelerated along the PPT electrodes [8, 9, 10], the electromagnetic component of the impulse bit was estimated by the following equation:

$$(I_{bit})_{EM} = \frac{\mu h}{2w}\int_o^t I^2(t)dt \qquad (3)$$

where μ is the permeability of free space and is equal to $4\pi \times 10^{-7}$ henries/m, h is the dimension of the plasma discharge in the direction normal to the thruster's exit plane and is set equal to 2.54 cm, w is the width of the discharge and it is set equal to 2.54 cm, and I(t) is the PPT current waveform which was experimentally measured. $(I_{bit})_{EM}$ values are presented in Table II and are plotted as a function of the discharge energy in Figure 9. In general, the electromagnetic component was directly proportional to the discharge energy and was nearly constant for all propellants at a given energy due to the almost identical current waveforms.

The fraction of the ablated mass that is electromagnetically accelerated, α, was determined from results from equation 3 and the following equation:

$$(I_{bit})_{EM} = M\alpha V \qquad (4)$$

where M is the experimentally measured ablated mass and V is the exhaust speed of ionized Teflon. V was assumed to be 40,000 m/sec [11]. α values for the different propellants at the different discharge energies are tabulated in Table II and are plotted in Figure 10. α values for nominal and high-density Teflon increase from about 20% to 33% for energy levels ranging from 5 to 60 joules, respectively. For porous Teflon, α ranges from 16% to 24% for energy levels ranging from 10 to 60 joules, respectively. Finally, for the 2%-carbon-impregnated Teflon, α ranges from 30% to 38% for energy levels ranging from 40 to 60 joules, respectively. In general, it was observed that for all propellants, increasing thruster energy increased the fraction of mass that was electromagnetically accelerated. This improved thruster efficiency due to a more efficient mass utilization, achieved by accelerating the ablated mass to higher average exhaust speeds under the influence of the JxB Lorentz force. Comparing α values for the different propellants, porous Teflon, with the lowest α among all the propellants tested, has the lowest thruster efficiency, whereas, carbon-impregnated Teflon, with the highest α, has the highest thruster efficiency.

Once α has been determined from equations 1 and 2, an average neutral speed C also were computed using the following equation:

$$(I_{bit})_{\exp} = M(1-\alpha)\bar{C} + M\alpha V \qquad (5)$$

Computed C values range between 3000 to 5000 m/sec, which agrees with earlier experimental findings [11].

Conclusions

Several different materials were evaluated as potential propellants in an ablative pulsed plasma thruster. The propellants, such as various density Teflon and carbon-impregnated Teflon were characterized and compared to nominal Teflon. Ablation rates, steady-state thrust, and impulse bit per pulse were measured for selected propellants over a range of number of pulses and discharge energies. Ablation rates for nominal Teflon ranged from 4.5 to 74.1 μg/pulse. Application of a least square linear fit to the ablation data resulted in a slope of 1.37 μg/joule for nominal Teflon, 1.37 μg/joule for high-density Teflon, 1.88 μg/joule for porous Teflon, and 1.12 μg/joule for 2%-carbon Teflon. The thrust or impulse bit per pulse agreed to within ±10% for all propellants over the range of energies tested. For nominal Teflon and high-density Teflon, efficiency ranged from 6 to 12%, for porous Teflon efficiency ranged from 7 to 13%, while for 2%-carbon Teflon efficiency ranged from 6 to 18%. Analysis of experimental results using zeroth-order slug modeling indicates that carbon-impregnated Teflon has the highest fraction of its ablated mass accelerated electromagnetically.

Insights into the propellant ablation process were gained with the examination of the experimental data. Ablation rates changed with propellant porosity, whereas thrust did not. These findings alone suggest that some propellant loss mechanism, which does not contribute significantly to thrust, was influenced by the changes in porosity. Both macroparticle ejection

and slow neutral evaporation (late time ablation) offer plausible explanations to the observed trends.

In order to incorporate any new propellant into a PPT system, extended life demonstrations must be completed. Operation of a PPT over at least one million pulses would identify any propellant feed issues associated with a change in propellant type. Also life demonstrations would alleviate concerns regarding the carbonization or sooting of the propellant surface, which can occur over long periods of operation.

Acknowledgements

The authors would like to acknowledge the efforts of Michael Swiatek and Frank Madi from the Facilities and Test Engineering Division and James Nichols, James Coy and Donna Neville from the Test Installation Division, who have contributed greatly to PPT testing activities.

References

[1] Burton, R.L. and Turchi, P.J., "Pulsed Plasma Thruster," Journal of Propulsion and Power, Vol. 14, Num. 5, pp 716-35, Sept.-Oct., 1998.

[2] Deininger, W.D., Weiss, M.A., Wiemer, D.J., Hoffman, C.N., Cleven, G.C., Patel, K.C., Linfield, R.P., Livesay, L.L., "Description of the StarLight Mission and Spacecraft Concept," Paper ID 277, 2001 IEEE Aerospace Conference, March 10-17, 2001.

[3] Blandino, J.J., Cassady, R.J., Sankovic, J.M., "Propulsion Requirements and Options for the New Millennium Interferometer (DS-3) Mission," AIAA-98-3331, July 1998.

[4] Benson, S.W., Arrington, L.A., Hoskins, W.A, and Meckel, N.J., "Development of a PPT for the EO-1 Spacecraft," AIAA-99-2276, June 1999.

[5] Ruchti, C.B., and Niemeyer, L., "Ablation Controlled Arc," IEEE Transactions on Plasma Science, Vol. PS-14, No. 4, August 1986.

[6] Arrington, L.A., Haag, T.W., Pencil, E.J. and Meckel, N.J., "A Performance Comparison of Pulsed Plasma Thruster Electrode Configurations," IEPC-97-127, also NASA TM-97206305, August 1997.

[7] Haag, T.W., "PPT Thrust Stand," AIAA-95-2917, also NASA TM-107066, July 1995.

[8] Jahn, R.G., Physics of Electric Propulsion, McGraw Hill Book Company, New York, 1969.

[9] Vondra, R.J., and Thomassen, K.I., "Performance Improvements in Solid Fuel Microthrusters," Journal of Spacecraft and Rockets, Vol. 9, No. 10, Oct. 1972, pp. 738-742.

[10] Humble, R.W., Henry, G.N., and Larson, W.J., Space Propulsion Analysis and Design , Chapter 9 (Electric Rocket Propulsion Systems, Peter J. Turchi), New York, 1995.

[11] Vondra, R.J., Thomassen, K., and Solbes, A., "Analysis of Solid Teflon Pulsed Plasma Thruster," Journal of Spacecraft and Rockets, Vol. 7, No. 12, Dec. 1970, pp. 1402-1406.

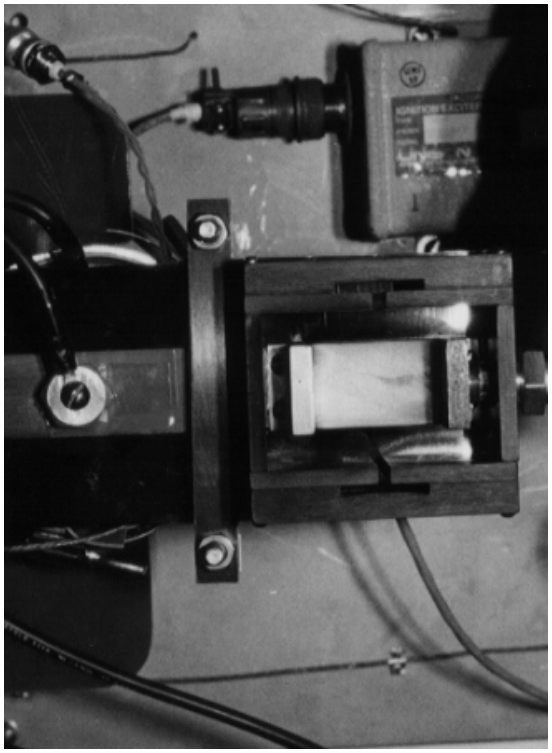

Figure 1 – Parallel plate pulsed plasma thruster.

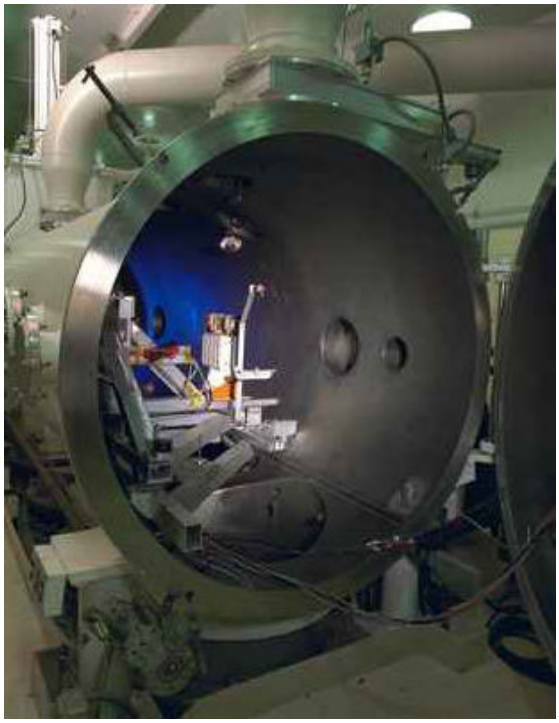

Figure 2 – Torsional-type impulse thrust stand installed in vacuum facility.

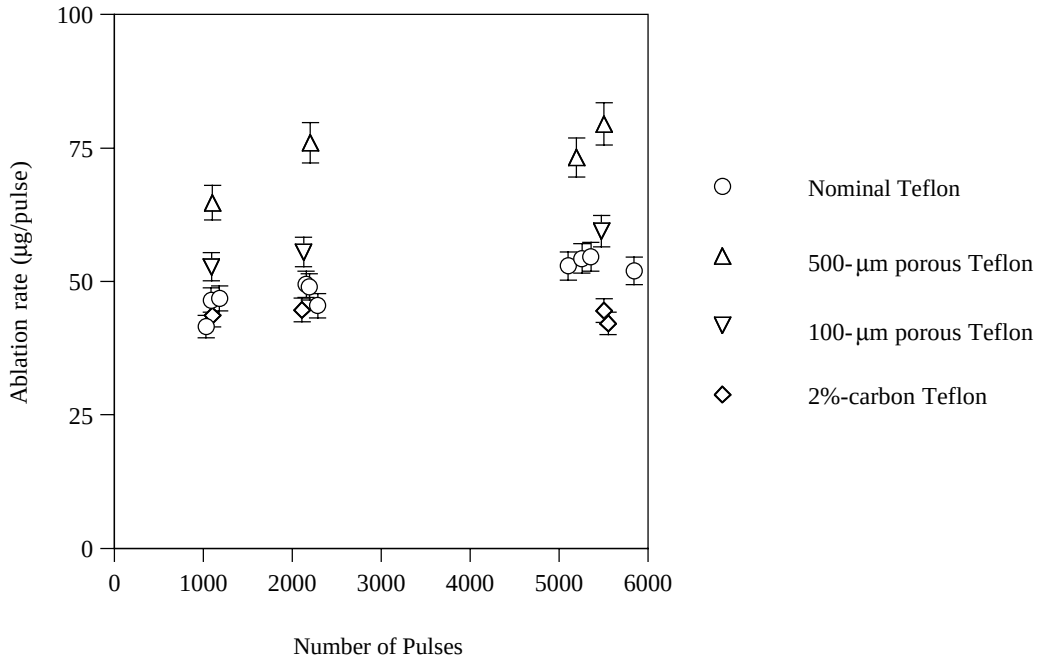

Figure 3 – Ablation rate as a function of number of pulses for selected propellants at 40 Joules.

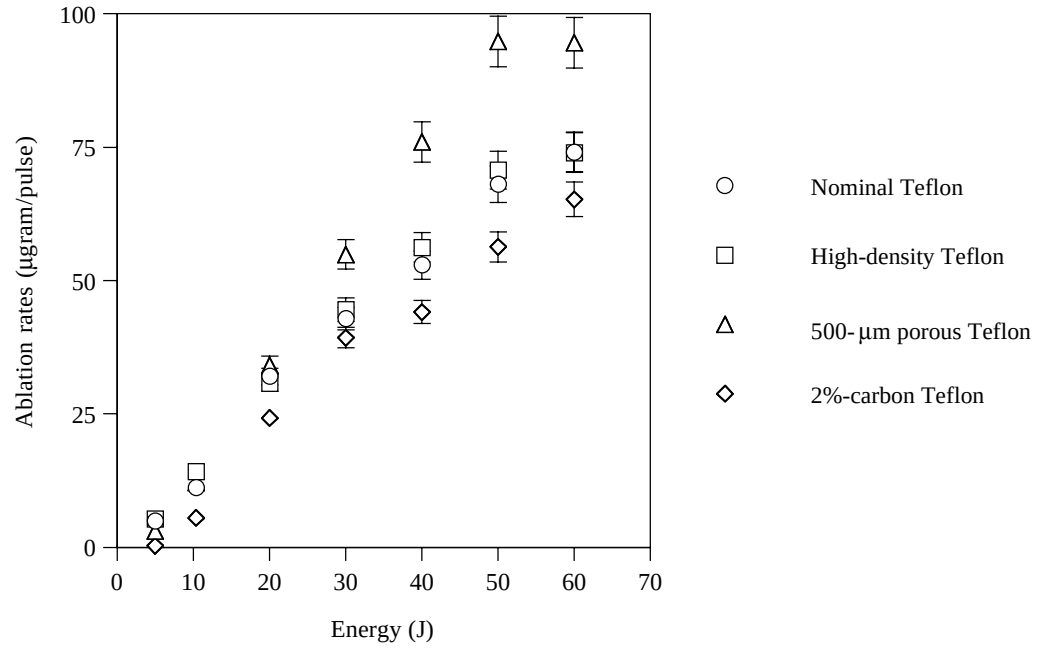

Figure 4 – Ablation rates as a function of energy for selected propellants.

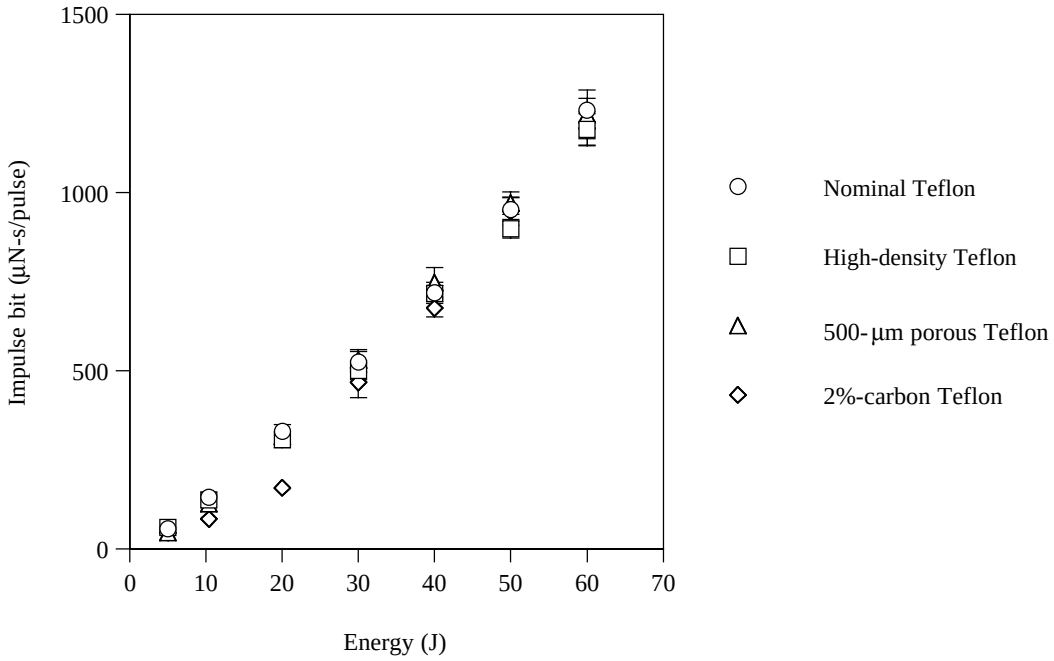

Figure 5 – Impulse bit as a function of energy for selected propellants.

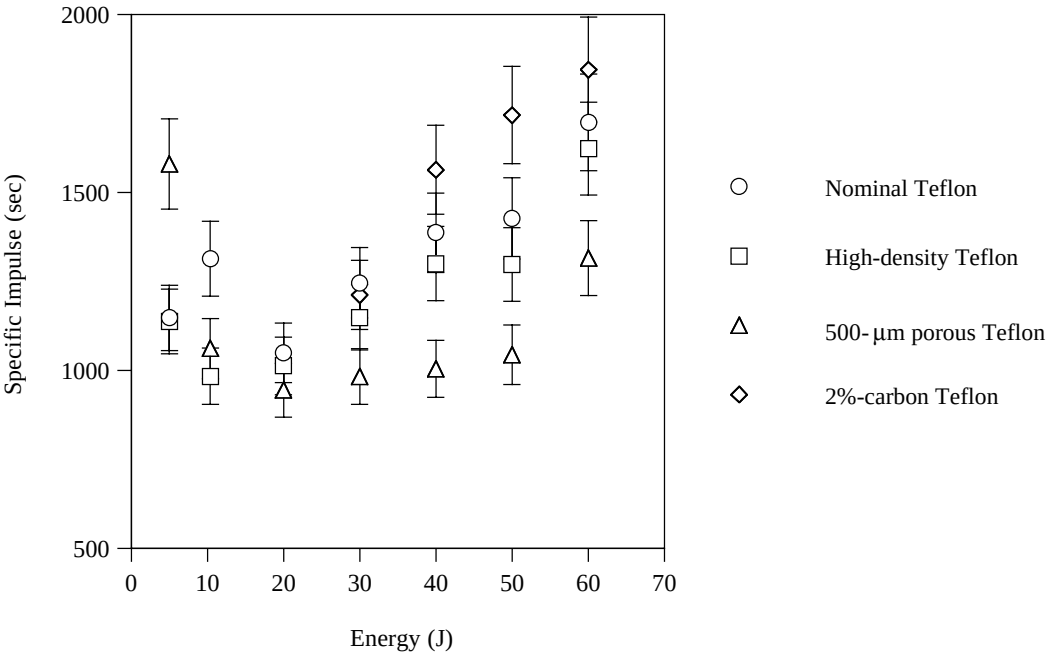

Figure 6 – Specific impulse as a function of energy for selected propellants.

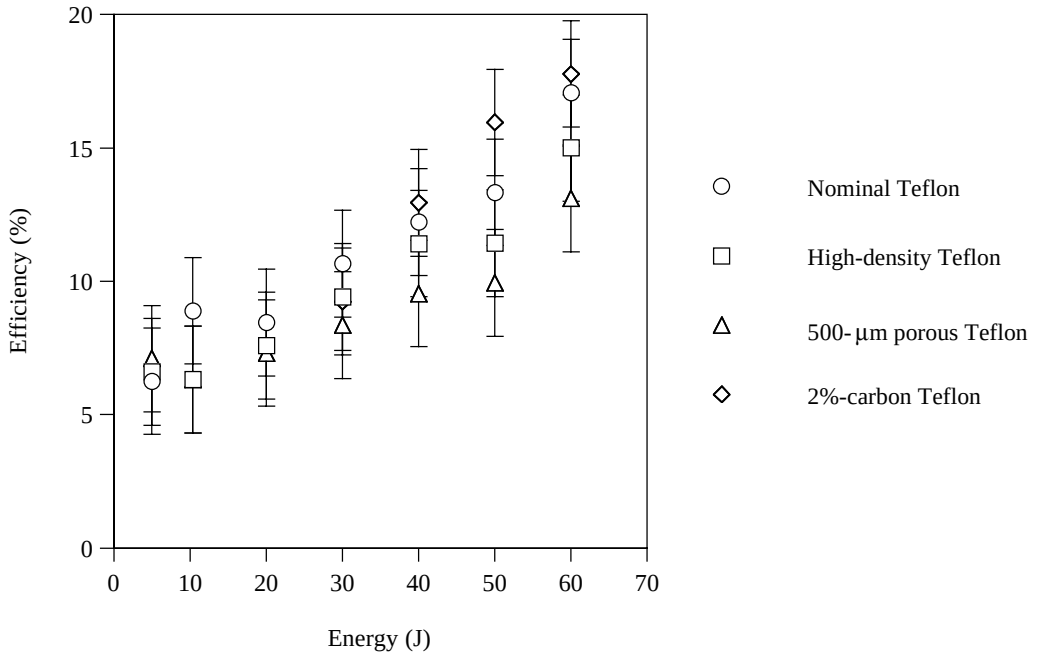

Figure 7 – Efficiency as a function of energy for selected propellants.

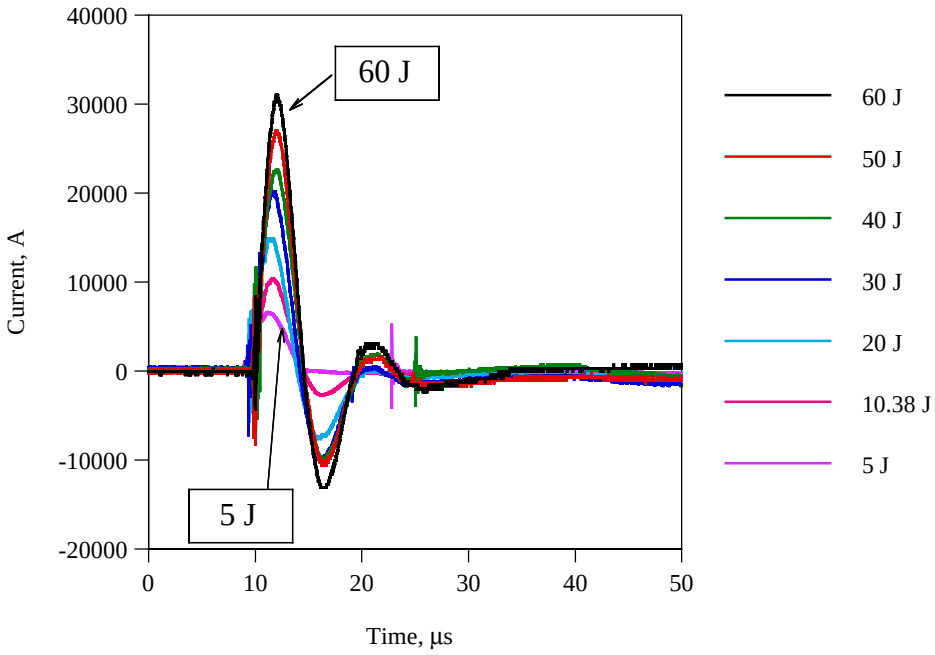

Figure 8 – Current waveforms for all energies for nominal Teflon.

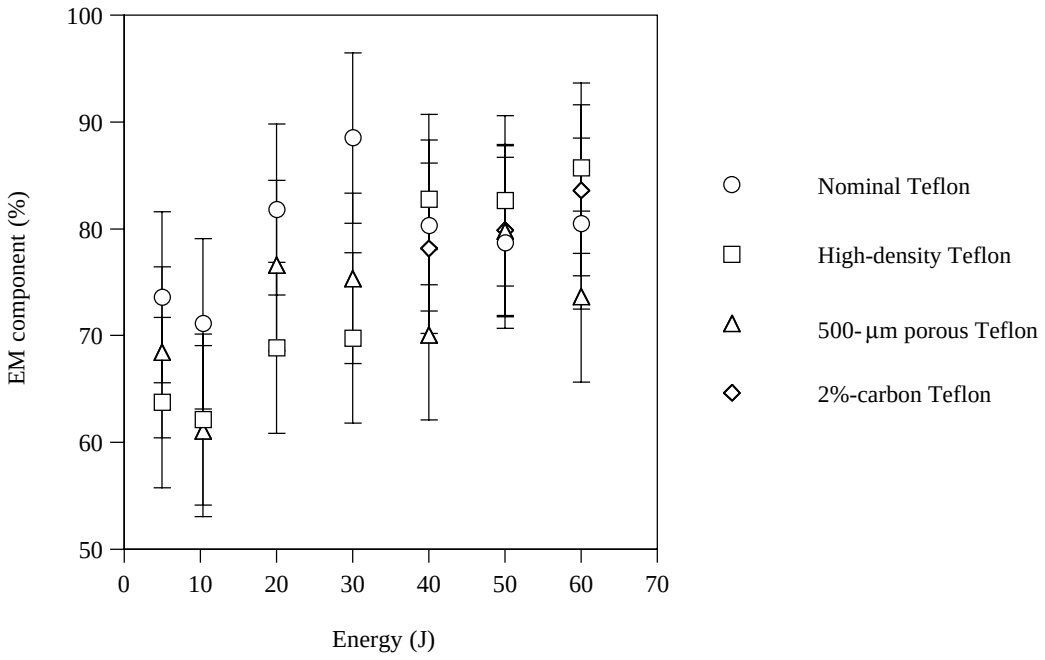

Figure 9 – Electromagnetic component as a function of energy for selected propellants.

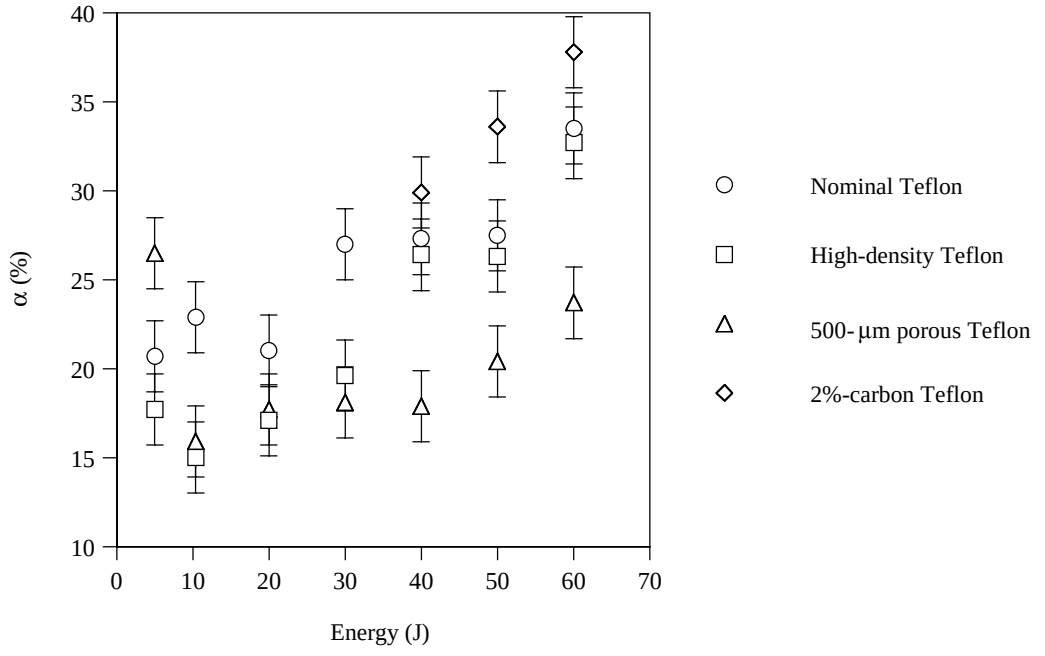

Figure 10 – Ablated mass electromagnetically accelerated (α) as a function of energy for selected propellants.

Table I – Propellant ablation rate test results.

Propellant	Energy (J)	Duration (pulses)	Ablation Rate (μg/pulse)
Nominal Teflon	5	1018	4.519
	5	2266	4.942
	5	5178	0.5214
	10.38	1032	12.21
	10.38	2050	10.24
	10.38	5237	11.13
	20	1047	27.13
	20	5318	32
	30	5002	42.84
	40	1087	46.5
	40	1180	46.8
	40	1030	41.55
	40	2155	49.4
	40	2191	49
	40	2287	45.47
	40	5849	52
	40	5260	54.3
	40	5361	54.62
	40	5105	52.89
	50	5114	68.07
	60	1060	73.58
	60	1000	72.2
	60	1052	73
	60	2316	74.09
	60	1994	74.92
High-density Teflon	5	5000	5.312
	10.38	4979	14.12
	20	5055	30.78
	30	5008	44.55
	40	5066	56.22
	50	5060	70.69
	60	2016	76.98
500-μm Porous Teflon	5	4996	2.96
	10.38	4619	12.12
	20	4950	34.12
	30	5861	54.87
	40	1101	64.7
	40	2203	76
	40	5508	79.5
	40	5198	73.24
	50	4882	94.81
	60	1940	94.59
100-μm Porous Teflon	40	1092	52.7
	40	2129	55.5
	40	5479	59.4
2%-carbon Teflon	5	4914	0.3
	10.38	4930	5.5
	20	4896	24.18
	30	5231	39.3
	40	1103	43.6
	40	2111	44.6
	40	5508	44.5
	40	5554	42.1
	50	5105	56.3
	60	2177	65.2

Table II – Thrust measurements and performance analysis results.

Propellant	Energy J	Ablation Rate µg/pulse	Impulse Bit (single pulse) µN-s/pulse	Thrust µN	Impulse Bit (continuous) µN-s/pulse	Specific Impulse seconds	Efficiency %	Electromagnetic Component %	Alpha %
Nominal Teflon	5	4.94	55.59	53.88	53.72	1147.8	6.25	73.6	20.7
	10.38	11.13	143.34	138.94	152.21	1314.2	8.89	71.1	22.9
	20	32	328.87	318.78	349.19	1048.7	8.45	81.8	21.0
	30	42.84	523.11	507.06	564.07	1246.0	10.6	88.5	27.0
	40	52.89	718.7	696.64	787.91	1386.6	12.2	80.3	27.3
	50	68.07	952.46	923.22	1029.65	1427.8	13.3	78.7	27.5
	60	74.09	1232	1193.95	1163.95	1696.4	17.1	80.5	33.5
High-density Teflon	5	5.312	59.18	58.55	50.23	1136.8	6.59	63.7	17.7
	10.38	14.12	136.05	134.59	142.33	983.2	6.31	62.1	15.0
	20	30.78	305.43	302.15	326.52	1012.6	7.58	68.9	17.1
	30	44.55	501.33	495.96	519.08	1148.3	9.40	69.8	19.6
	40	56.22	716.29	708.61	720.01	1300.1	11.4	82.7	26.4
	50	70.69	898.59	888.95	920.95	1297.1	11.4	82.6	26.3
	60	76.98	1176.81	1164.19	1139.63	1623.2	15.0	85.7	32.7
500-µm Porous Teflon	5	2.96	45.83	45.83	26.07	1579.9	7.10	68.4	26.5
	10.38	12.12	126.03	124.68	130.37	1061.1	6.31	61.0	15.9
	20	34.12	315.8	312.41	330.27	944.4	7.31	76.6	17.7
	30	54.87	528.48	522.81	547.55	982.8	8.35	75.4	18.1
	40	73.24	747.6	739.59	747.45	1003.8	9.54	70.1	17.9
	50	94.81	970.3	959.91	982.12	1044.3	9.93	79.8	20.4
	60	94.59	1219.5	1206.43	1199.4	1315.6	13.1	73.6	23.7
2%-carbon Teflon	5	0.3	44.71	43.34	NA	NA	NA	NA	NA
	10.35	5.5	82.94	80.39	62.07	NA	NA	NA	NA
	20	24.2	170.92	165.68	239.43	NA	NA	NA	NA
	30	39.3	466.62	452.29	496.59	1211.6	9.23	NA	NA
	40	44.1	675.76	655.02	718.28	1563.6	12.9	78.2	29.9
	50	56.3	947.66	918.57	966.57	1717.6	16.0	79.9	33.6
	60	65.2	1179.16	1142.97	1188.26	1845.4	17.8	83.6	37.8